Digital imaging-based colourimetry for enzymatic processes in transparent liquid marbles.

ChemPhysChem

Chemistry Europe
European Chemical Societies Publishing

Accepted Article

Title: Digital imaging-based colourimetry for enzymatic processes in transparent liquid marbles

Authors: Nhat-Khuong Nguyen, Pradip Singha, Jun Zhang, Hoang-Phuong Phan, Nam-Trung Nguyen, and Chin Hong Ooi

To be cited as: *ChemPhysChem* 10.1002/cphc.202000760

Link to VoR: https://doi.org/10.1002/cphc.202000760

WILEY-VCH

10.1002/cphc.202000760

WILEY-VCH

ARTICLE

Digital imaging-based colourimetry for enzymatic processes in transparent liquid marbles

Nhat-Khuong Nguyen[a], Pradip Singha [a], Jun Zhang[a], Hoang-Phuong Phan[a], Nam-Trung Nguyen*[a], Chin Hong Ooi*[a]

[a] N.-K. Nguyen, P. SIngha, Dr. J. Zhang, Dr. H.-P. Phan, Prof. N-T. Nguyen, Dr. C.H. Ooi
Queensland Micro- and Nanotechnology Centre, Griffith University,
170 Kessels Road, Nathan 4111 Queensland, Australia
E-mail: nam-trung.nguyen@griffith.edu.au, c.ooi@griffith.edu.au

Abstract: Liquid marble is a promising microreactor platform that recently attracts significant research interest owing to their ability to accommodate a wide range of micro reactions. However, the use of destructive and ex-situ methods to monitor reactions impairs the potential of liquid-marble-based microreactors. This paper proposes a non-destructive, in situ, and cost-effective digital-imaging-based colourimetric monitoring method for transparent liquid marbles, with the example of the enzymatic hydrolysis of starch. The colourimetric reaction between starch and iodine produces a complex that exhibits a dark blue colour. We found that the absorbance of red channel of digital images showed a linear relationship with starch concentration with high sensitivity and repeatability. This digital-imaging based-colourimetric method was used to study the hydrolysis of starch by α-amylase. The results showed high accuracy and applicability of first-order kinetic for this reaction. The demonstration of digital-imaging-based colourimetry indicates the potential of liquid marble-based microreactors.

1. Introduction

Chemical reactors can be categorised into batch or continuous reactors. In continuous reactors, reactant introduction and product extraction occur simultaneously. Continuous reactors are preferred in large-scale productions as they can deliver higher reaction efficiencies and lower cost [1-3]. Conversely, batch reactors offer flexibility for small-scale operations. Batch reactors can conveniently accommodate reactions with various reaction times and reaction phases that are not feasible in continuous reactors. In recent decades, the miniaturisation of reactors has attracted enormous interests owing to their superior properties. Microreactors enhance mass and heat transfer which increases reaction kinetics and improves yield as compared to the macroscale counterparts [4-6]. Owing to these advantages, microreactors, especially microfluidic reactors have attracted tremendous research interests [7-12]. Nevertheless, there is a lack of effort to scale down batch reactors. A liquid marble is a droplet covered with hydrophobic particles [13-14]. Recently, the liquid marble emerged as a promising microscale batch reactor platform. The coating particles prevent direct contact between the interior liquid and surrounding substrates, allowing the liquid marble to avoid wetting and contamination. The liquid marble has a volume ranging from sub-microlitres to sub-millilitres. The combination of numerous interior liquids and coating particles can render liquid marbles with highly specific properties [15]. Liquid marbles are also highly versatile and can be manipulated using electrostatics [16-19], magnetism [20-22], thermal gradient, and surface tension gradient [23-25]. These properties enable tailor-made microreactor platforms, making liquid marbles an excellent candidate for a microscale batch reactor.

Enzymatic starch hydrolysis is an important process in the production of foods, biofuels and pharmaceuticals [26-28]. This process also finds various applications in analytical chemistry for the determination of starch content or enzyme activity [29-32]. The reaction kinetics of enzymatic starch hydrolysis is well-studied for macroscale reactors [33-36]. Recently, microscale enzymatic starch hydrolysis was demonstrated by immobilising enzyme into continuous microfluidic reactors [37, 38]. However, the high viscosity of starch solution during gelatinisation leads to inefficient mixing in microchannel-based reactors [39, 40]. Furthermore, these reactors are also susceptible to enzyme leakage and enzyme contamination. Complex procedures are required to fabricate these immobilised enzyme reactors, significantly reducing their potential applications. A highly versatile microreactor platform such as the liquid marble can overcome these drawbacks. The present work utilises a liquid marble-based microreactor to accommodate enzymatic starch hydrolysis for the first time. Liquid marble-based microreactors are insusceptible to inefficient mixing of solvents with viscosity higher than 40 MPa.s [39]. The small volume of liquid marbles also reduces reagent and energy consumption of enzymatic reactions.

This paper also addresses the limitations associated with liquid marble-based microreactors such as the inability to monitor reactions. Most prior works utilised destructive methods such as ultraviolet-visible (UV-vis) spectrophotometry [41, 42] or proton nuclear magnetic resonance (^{1}H NMR) spectroscopy [43] for quantitative analysis of the reacted products. Non-destructive monitoring methods were also reported such as on-line electrochemical detection of liquid contents within a liquid marble coated with magnetic particles [44]. This method suffers from potential contamination as the liquid content was continuously exposed to the surrounding environment during the measurement. Another monitoring strategy is using a combination of ultrasensitive surface-enhanced Raman scattering (SERS) and plasmonic liquid marbles [45]. These methods require highly specialised coating particles and expensive equipment. Oliveira et al. utilised low-cost digital imaging-based colourimetry to monitor the reactions in liquid marbles [46]. However, the opaqueness of coating particles of liquid marbles can significantly impact the potential for optical analysis of interior liquids. Therefore, the emergence of transparent liquid marble provides a promising platform for real-time and continuous monitoring of reactions such as cell culture [47]. This paper used transparent

liquid marbles and digital image-based colourimetry for a non-destructive, in situ and cost-effective monitoring of starch hydrolysis for the first time.

2. Theoretical background

Digital imaging-based colourimetric method has been employed as a cost-effective alternative for a spectrophotometer in quantitative analysis in previous studies [48-52]. These methods are based on the Beer-Lambert law which establishes the relationship between light absorption and concentration of the sample being investigated [53]:

$$A = K \times C \times L \quad (1)$$

where *A* is the light absorbance, *K* is the molar absorptivity, *L* is the optical path length and *C* is the concentration of the compounds. Absorbance can be obtained empirically as follows:

$$A = -\log\left(\frac{I}{I_0}\right) \quad (2)$$

where I_0 and *I* are respectively the intensities of light before and after passing through the compound. The concentration of a compound can be determined by measuring its light absorbance with a constant molar absorptivity and optical path length [54]. Beer-Lambert law was well adapted to digital imaging as the colours of the captured images are given by the diffuse reflection of incident radiation that was not absorbed by the compounds. In the red, green, and blue (RGB) model, intensities of the three colour channels are used to form a single colour in one pixel. Therefore, it is feasible to establish a relationship between the colour components and the concentration of the analyte [55]. For the RGB model, the intensity is now defined as the pixel values of the individual colour channels and RGB absorbance is defined as $-\log(I/I_0)$ where I and I_0 are the intensity of the sample being investigated and intensity of the blank sample respectively [48].

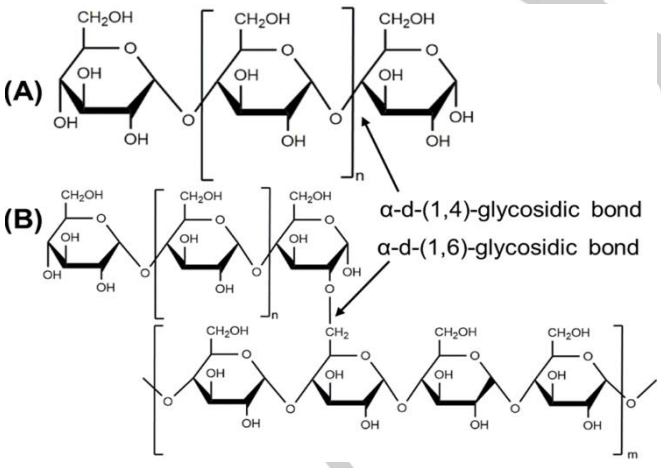

Figure 1. The structures of the two main components of starch: (A) amylose and (B) amylopectin

Starch is a polysaccharide consisting of two main components, amylose and amylopectin as shown in Figure 1. Amylose is a polymer consisting of several hundred to thousand α-D-glucose units bound together by α-d-(1,4)-bonds. Amylopectin is a highly branched polymer, consisting of relatively short branches of 20 to 25 units of α-D-glucose linked by α-d-(1,4) -bonds and connected by α-d-(1,6)-glycosidic linkages. When in contact with iodine, amylose forms a helical inclusion complex which exhibits a deep blue colour, having a maximum absorbance peak of around 620 nm [56]. Since this wavelength strongly correlates with the colour red [57], we expect that the intensity of the red channel to be highly sensitive to the concentration of starch. On the other hand, when being hydrolysed by α-amylase, internal α-d-(1,4)-glycosidic bonds of the long-chain saccharides break down, producing various hydrolysates including maltotriose, maltose, and dextrins. As the concentration of starch decreases, the dark blue colour fades. Hence, the colour can be monitored to quantify the starch concentration.

Silica nanoparticle-coated liquid marbles are highly transparent and allow for the observation of the interior liquids, thus we expect that the liquid marble coated with this material can be used for digital-imaging colourimetry. However, the evaporation rate of the liquid marble needs to be characterised as it may affect the liquid marble shape, volume, and concentration of its constituents [58-60]. Since the change in sample volume will affect the analysis of the results similar to the change of optical path length in spectrophotometry, it is important to choose a suitable working timeframe and temperature to minimise the effect of evaporation.

Experimental Section

Liquid marbles reported in this study were formed using soluble starch solution as interior liquid and hydrophobic fumed silica treated with D4 (Octamethylcyclotetrasiloxane) (AEROSIL® R 106, ≥ 99.8 % silica, Evonik) as coating powder. Soluble starch solution was prepared by adding deionised (DI) water (10 mL) to soluble starch (0.5 g, Sigma-Aldrich product S9765) to form a smooth paste. This paste was added into DI water (70 mL) at 80 to 90 °C and stirred for 1 hour. A stock solution of starch (5mg.mL^{-1}, 100 mL) was formed by further addition of DI water. This stock solution was further diluted to make a solution (0.25 mgmL^{-1}) to be used in hydrolysis kinetic study. Fresh starch solution was prepared every run to avoid starch retrogradation. The starch solution was then deposited on a hydrophobic fumed silica powder bed. The droplets were gently rolled on the dish to coat it with silica particles. After formation, liquid marbles were transported to a clean weighing boat without powder and rolled gently to remove any excess particles.

In order to investigate the evaporation rate of silica liquid marble, liquid marbles (80 µL) containing starch solution (0.25 mgmL^{-1}) were placed in room temperature 20 °C and relative humidity of 38 %. Side views of liquid marbles were recorded with a camera (Ximea xiQ - USB3 MQ013CG-ON) and a telecentric lens (Edmund Optics 63074, 0.5X) to study the change in volume for 5 minutes. The volume of liquid marble was determined using Drop Analysis – Low-bond axisymmetric drop shape (LB – ADSA) plugin of the freely available ImageJ software [61].

α-Amylase from *Bacillus licheniformis* (Sigma-Aldrich product A3403, 19,272 units.mL^{-1}) was used in this study. Sigma-Aldrich defines a unit of activity (U) as that which liberates 1 mg of maltose in 3 minutes from starch at pH 6.9 and 20 °C. Three enzyme solutions with different concentrations (7.71 U.mL^{-1}, 9.64 U.mL^{-1} and 11.56 U.mL^{-1}) were prepared to be used in hydrolysis kinetic study.

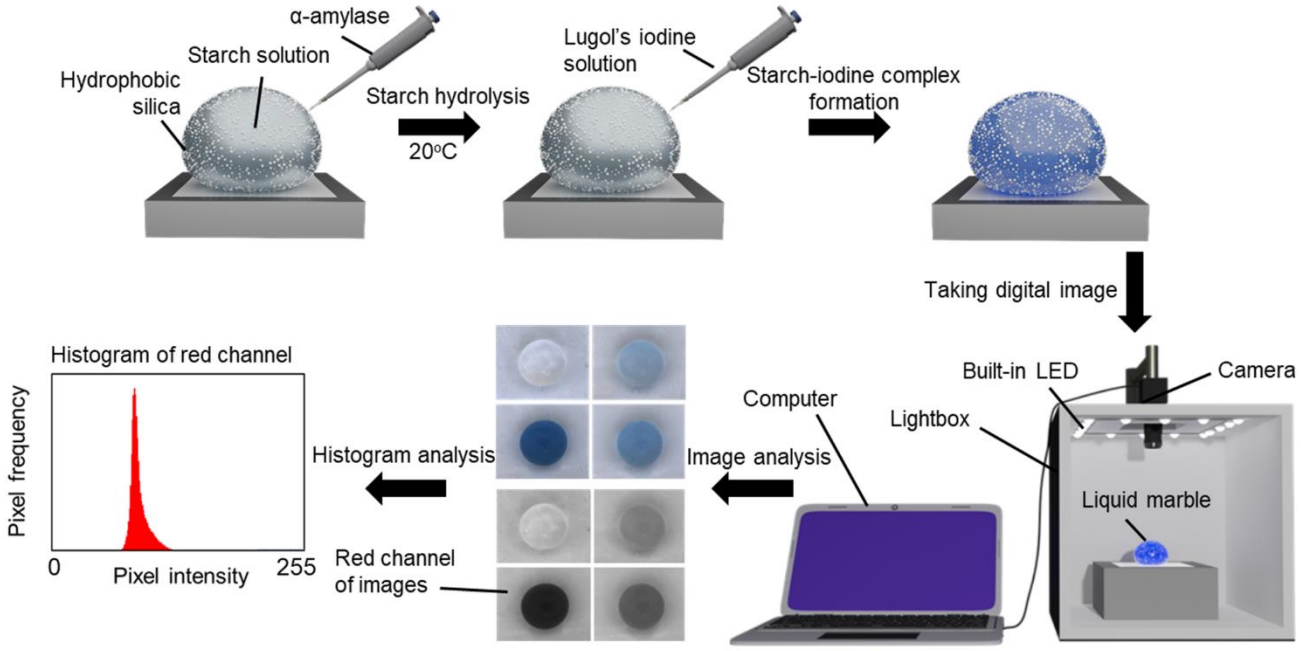

Figure 2. Experimental procedure for digital-imaging based colourimetry to monitor the enzymatic hydrolysis of starch in liquid marbles.

Hydrolysis of starch in liquid marbles was conducted by injecting the prepared α-Amylase solutions (3μL) into liquid marbles containing starch solution (0.25 mg.mL^{-1}, 77μL). Three different enzyme concentrations (7.71 U.mL^{-1}, 9.64 U.mL^{-1} and 11.56 U.mL^{-1}) were investigated respectively. After 1 to 5 minutes, Lugol 's iodine indicator (3.2 μL, Sigma-Aldrich product 62650, diluted 10 times with DI water) was injected and the liquid marbles turned blue with a colour saturation that depends on the concentration of the remaining starch. The colour of liquid marble was recorded and monitored to investigate the reaction kinetics of starch hydrolysis. Reactions were carried out in a short duration of 5 minutes and room temperature of 20 °C to mitigate the effects of evaporation. Separate liquid marbles were used for every time step.

Digital images of liquid marbles were taken in a lightbox as shown in Figure 2 in order to maintain the stability of environmental light and photographic conditions. The camera (Ximea xiQ - USB3 MQ013CG-ON) and lens (Edmund Optics 63074, 0.5X) setup was mounted on top of the lightbox to obtain the top view of the liquid marble. This camera uses 8 bit for each colour channel which corresponds to 256 possible levels. Digital images of liquid marbles were analysed using the freely available ImageJ software. We first split the images into 3 colour channels of red, green and blue. The mean intensity of each channel of the top view was measured. The absorbance of each sample was calculated by taking the common logarithm of the ratio between the intensity of the blank sample and the sample being analysed. Next, we constructed calibration curves to determine the concentration of the samples.

3. Results and discussion

This section discusses the use of digital imaging method to monitor enzymatic hydrolysis of starch in liquid marble-based microreactors. First, we discuss the transparency and the effect of evaporation on liquid marbles. Subsequent sections report the use of digital-imaging-based method for the quantification of starch concentration and study of reaction kinetics.

3.1 Transparent liquid marble and evaporation

Figure 3(A) and 3(B) show the images of liquid marbles (60 μL) covered with fumed silica nanoparticles and PTFE. Silica nanoparticles exhibited excellent optical transparency compared to the micrometre-sized PTFE coating. This can be explained by the small particle size of AEROSIL® R 106, ranging from 10 to 20nm, leading to smaller agglomerates with median diameters less than 0.4μm [62] which allows for better light transmittance than PTFE microparticles with a nominal diameter of 1μm. Oliveira et al. reported the use of micrometre-sized silica coating particles for digital imaging but the translucency of the material could interfere in the results [46]. Therefore, AEROSIL® R 106 silica nanoparticle is a more suitable coating material for this method. Our liquid marbles coated with AEROSIL® R 106 also possess high apparent contact angles of more than 157°, Figure 3(C), which demonstrates the high hydrophobicity of the coating particle.

It is important to determine a working temperature and reaction time for the experiments to mitigate the evaporation of interior liquid in liquid marble which can lead to a change in the concentration of components during the course of reaction. Figure 3(D) shows that the normalised volume of liquid marble decreased to 97.5 % at a temperature of 20 °C and relative humidity of 38 % over a period of 5 minutes, retaining almost the same shape and dimension. The small change of less than 2.5 % in liquid marble volumes posed a negligible effect and did not significantly affect the enzyme concentration or colourimetric results. Hence, we chose this temperature and reaction time to study starch concentration and enzymatic starch hydrolysis. Larger liquid marbles can further mitigate the effect of evaporation but they were difficult to handle during transfer.

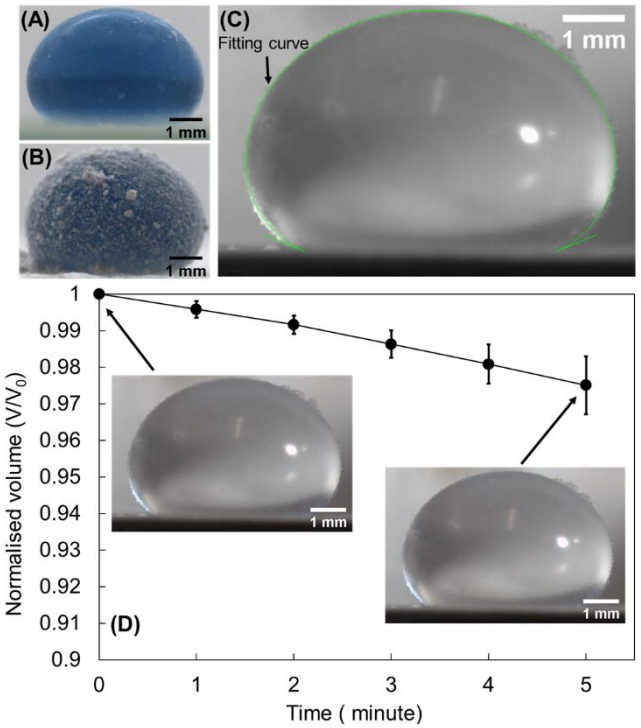

Figure 3. Liquid marbles (60 µL) covered with (A) fumed hydrophobic silica nanoparticles and (B) Polytetrafluoroethylene (PTFE) microparticles. (C) Apparent contact angle of a liquid marble (80 µL) containing starch solution coated with fumed hydrophobic silica nanoparticles. (D) Normalised volume liquid marble over a period of 5 minutes at 20 °C, and relative humidity of 38 %. All runs were conducted with an initial marble volume of 80 µL.

3.2 Quantification of starch concentration based on digital imaging colourimetry.

We constructed calibration curves based on the absorbance of red, green, and blue channels. The characterisation of the digital-imaging based method includes determining the sensitivity of linear regression curves, the repeatability, the limit of detection (LOD) and the limit of quantification (LOQ).

Figure 4(A) shows the images of the top view of liquid marbles (83.2 µL) containing different concentrations of starch solutions (80 µL) and Lugol's iodine indicator (3.2 µL) and their images in RGB channels, with the dark blue colour of starch liquid marbles becoming more saturated with the increase of starch concentration from 0 to 0.24mg.mL^{-1}. Figure 4(B) indicates the intensities of all three channels declining with the increase of concentration. The mean intensity of red channel decreased rapidly from 188.4 to 39.5 while the blue channel experienced a smaller decline from 208.5 to 112.1. The high sensitivity of red channel was expected as we have discussed that the amylose-iodine complex absorbs a maximum peak of around 620 nm. However, since amylopectin also forms a complex with iodine which absorbs a maximum wavelength at around 550nm which was formed from the red and green colour, the green channel was shown to have moderate sensitivity. Relative standard deviation was calculated to be less than 4.23%, 3.96% and 3.54% for R, G, B channel, respectively. These results show good repeatability of the proposed method.

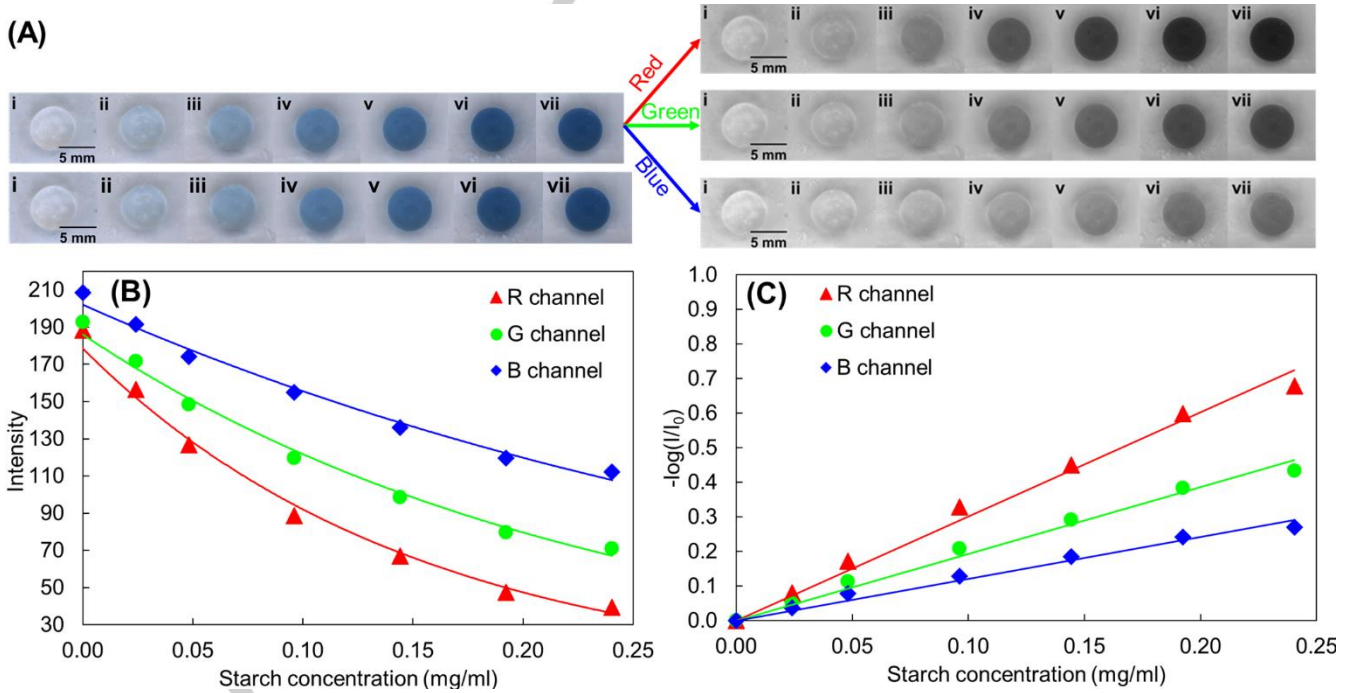

Figure 4. (A) Digital images of the top view of liquid marbles with different concentrations (i) 0mg.mL^{-1}, (ii) 0.024mg.mL^{-1}, (iii) 0.048mg.mL^{-1}, (iv) 0.096mg.mL^{-1}, (v) 0.144mg.mL^{-1}, (vi) 0.192mg.mL^{-1}, (vii) 0.24 mg.mL^{-1} and their images in RGB channels. Plots of (B) Intensity of R, G, B channel and (C) RGB absorbance -log(I/I$_0$) versus starch concentration. Images of every starch concentrations were taken with 3 separate liquid marbles and average intensity value was calculated.

From the intensities of the three channels, we constructed calibration curves based on RGB absorbance and starch concentration. Figure 4(C) shows the three calibration curves of the channels with the following linear regression equation:

$$-\log(I/I_0) = S \times [Starch]\ \text{mg.mL}^{-1} \quad (3)$$

where S is the slope of the fitted curve with values shown in the following table.

Table 1. Slope and R^2 value of the linear regression equation

	Red channel	Blue channel	Green channel
Slope	3.02	1.93	1.21
R^2	0.988	0.987	0.980

All the calibration curves show high linearity within the starch concentration range from 0 to 0.24mg.mL^{-1}, indicating strong agreement with the Beer-Lambert law. As shown in Table 1, the red channel exhibited higher sensitivity than the green and blue channel. The absorbance of red channel was used to determine the starch concentration for the hydrolysis experiments. It is worth to note that within the starch concentration range of 0.025–0.3 mg.mL^{-1}, the higher sensitivity of red channel compared to green and blue channel was also observed in a previous study of Shankar et al. [63].The limits of detection (LOD) and quantification (LOQ) were calculated using the following equations [64]:

$$\text{LOD} = 3 \times \frac{\sigma}{\beta} \quad (4)$$

$$\text{LOQ} = 10 \times \frac{\sigma}{\beta} \quad (5)$$

where σ is the standard deviation of absorbance of ten blank samples and β is the slope of the calibration curve. Thus, the LOD and LOQ were 0.007mg.mL^{-1} and 0.024mg.mL^{-1} respectively. The low LOD and LOQ show that this method is sensitive enough to work with low concentration analyte. Since many studies of liquid marbles as microreactors usually utilise methylene blue and other chemicals that can be quantitatively determined using spectrophotometry [65], digital imaging-based method is a promising and cost-effective alternative with high accuracy and reproducibility.

3.3 Demonstration of starch hydrolysis monitoring using colourimetric digital imaging

We demonstrated starch hydrolysis assay by injecting α-amylase into liquid marble containing starch solution. The absorbance of the red channel was measured, and Equation (3) was used to calculate the residual starch concentration.

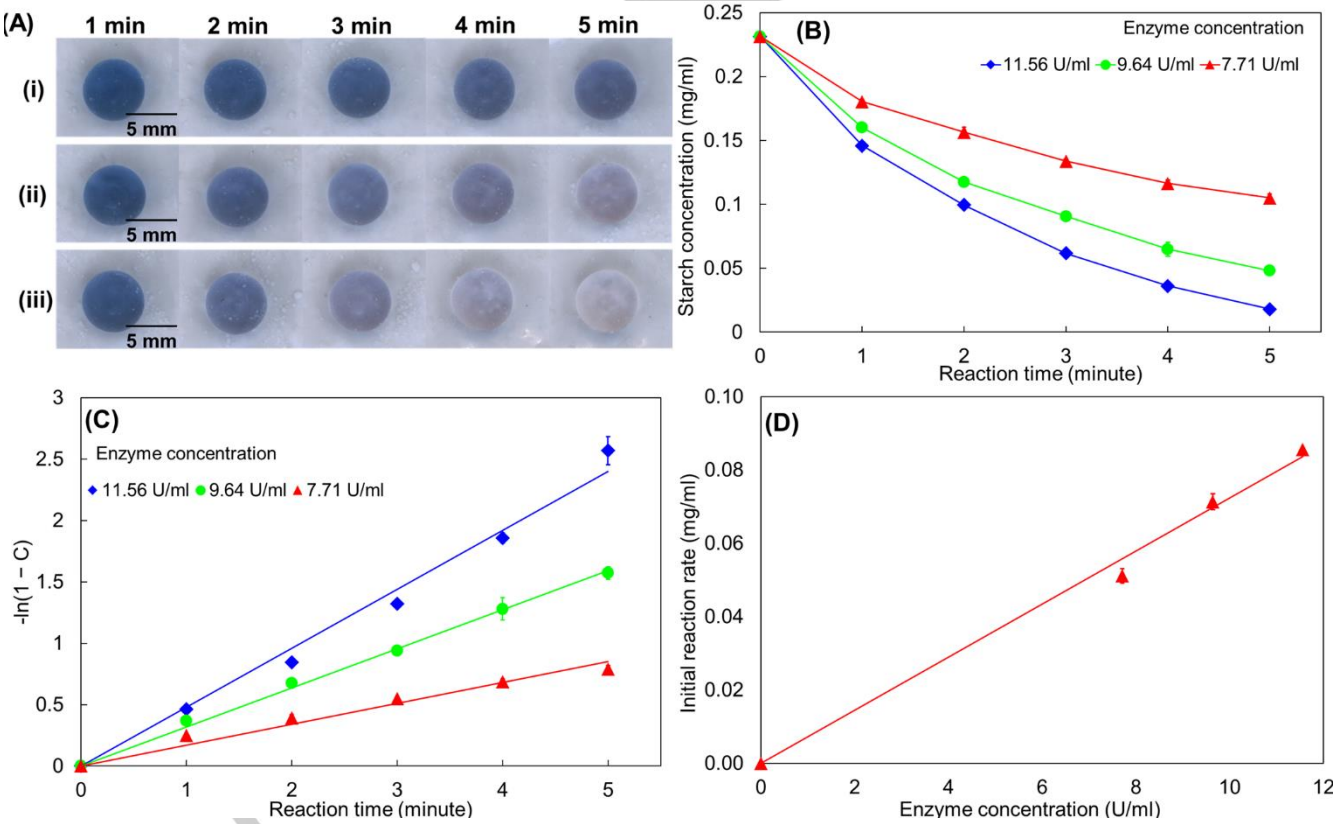

Figure 5. (A) Digital images depicting the top view of liquid marbles injected with different enzyme concentrations of (i) 7.71 U.mL^{-1}, (ii) 9.63 U.mL^{-1}, (iii) 11.56 U.mL^{-1} over a reaction time of 5 minutes. (B) Plot of residual starch concentration based on the absorbance of red channel versus reaction time. Images at one time point were taken with 3 different liquid marbles and the average absorbance value was calculated. (C) Plot of the value -ln(1 − C) versus reaction time with digestion rate constant as the slope of the fitting curve. (D) Plot of initial reaction rate versus concentration of enzyme.

Figure 5(A) shows that the dark blue colour of liquid marbles faded over time, indicating the decrease of starch concentration due to the hydrolysis processes. Higher concentrations of enzyme increased the fading rate. A plot of residual starch concentration versus reaction time was constructed, Figure 5(B). The starch concentration decreased rapidly initially then gradually slowed down. The reaction rate depends on residual starch concentration. We employed the first-order rate equation which was used in previous studies to investigate the digestibility kinetics [66]:

$$C = 1 - e^{-Kt} \quad (6)$$

where *C* is the percentage of starch digested at the time *t* and *K* is a digestion rate constant. The above equation can be transformed into:

$$-\ln(1 - C) = Kt \quad (7)$$

The digestion rate constants thus were obtained as the slope of the plot of value -ln(1−*C*) against time for each enzyme concentration. Figure 5(C) shows that all the fitting curves have high linearity with R^2 value higher than 0.967 indicating the suitability of applying first-order kinetics for starch hydrolysis processes. Digestion rate constants are calculated at 0.171, 0.319 and 0.480 min^{-1} for enzyme concentration of 11.56, 9.64 and 7.71 $U.mL^{-1}$ respectively, indicating enzyme concentration also significantly increases the reaction rate. Figure 5(D) shows the high linearity in the relationship the concentration of enzyme and reaction rate with an R^2 value of 0.993 which shows an agreement with previous studies [67, 68]. These results show that kinetics analysis conducted in conventional platforms such as test tubes, flasks or microplates can be carried out in liquid marble-based microreactor with high accuracy and repeatability [35, 69]. The amount of enzyme and indicator used for each experiment was only a few microlitres compared to millilitres used in test tubes or tens of microlitres as in microplate platform, significantly reducing the reagents required and waste generated. It is worth to mention that the proposed method is highly temperature-dependent since the effect of evaporation on liquid marbles becomes more significant at elevated temperature, leading to the change in concentration of reactants and products over the reaction period. Furthermore, the enzymatic reaction rates are sensitive to temperature. Therefore, it is important to determine a suitable working temperature to minimise the effect of evaporation.

4. Conclusion

We demonstrated a digital-imaging-based colourimetric method to monitor the enzymatic process in transparent liquid marbles. The high transparency of hydrophobic fumed silica nanoparticles enabled the observation of interior liquid. The red channel of digital images showed high sensitivity to starch concentration and a linear relationship between the absorbance of the red channel and the starch concentration was observed. Low LOD and LOQ of 0.007$mg.mL^{-1}$ and 0.024$mg.mL^{-1}$ were obtained respectively, showing that this method is sensitive enough to work with low concentration analytes. The kinetics of hydrolysis reaction was studied using this method showed high accuracy and applicability with the first-order kinetic. Liquid marbles as a reaction platform greatly reduce the amount of reagents and generated waste. Digital imaging-based colourimetry is a cost-effective, precise, non-destructive and in situ monitoring method that greatly enhances the potential of liquid marble-based microreactors platform.

Acknowledgements

C.H.O. acknowledges funding support from the Australian Research Council (ARC) Discovery Early Career Research Award (DECRA) DE200100119. N.T.N. acknowledges funding support from the ARC Discovery Project DP170100277. N.K.N. acknowledges funding support from the Griffith University International Postgraduate Research Scholarship and the ARC DECRA Postgraduate Research Scholarship.

Keywords: • digital imaging • liquid marble • microreactor • RGB model • starch hydrolysis• colourimetry

[1] Y. Wen, X. Wang, H. Wei, B. Li, P. Jin, L. Li, *Green Chem.* **2012**, *14*, 2868-2875.
[2] A. Corma, C. Martínez, F. Melo, L. Sauvanaud, J. Carriat, *Appl. Catal. A: Gen.* **2002**, *232*, 247-263.
[3] V. Shvets, V. Sapunov, R. Kozlovskiy, A. Luganskiy, A. Gorbunov, F. Sovetin, T. Gartman, *Chem. Eng. J.* **2017**, *329*, 275-282.
[4] A. Tanimu, S. Jaenicke, K. Alhooshani, *Chem. Eng. J.* **2017**, *327*, 792-821.
[5] P. Watts, S. J. Haswell, *Chem. Soc. Rev.* **2005**, *34*, 235-246.
[6] J. i. Yoshida, A. Nagaki, T. Yamada, *Chem. Eur. J.* **2008**, *14*, 7450-7459.
[7] A. J. Demello, *Nature* **2006**, *442*, 394-402.
[8] B. Su, S. Wang, Y. Song, L. Jiang, *Nano Res.* **2011**, *4*, 266-273.
[9] S. J. Haswell, P. Watts, *Green Chem.* **2003**, *5*, 240-249.
[10] P. T. Baraldi, V. Hessel, *Green Process. Synth.* **2012**, *1*, 149-167.
[11] P. Watts, C. Wiles, *J. Chem. Res.* **2012**, *36*, 181-193.
[12] Y.-F. Yap, S.-H. Tan, N.-T. Nguyen, S. S. Murshed, T.-N. Wong, L. Yobas, *J. Phys. D* **2009**, *42*, 065503.
[13] P. Aussillous, D. Quéré, *Nature* **2001**, *411*, 924-927.
[14] P. Singha, C. H. Ooi, N.-K. Nguyen, K. R. Sreejith, J. Jin, N.-T. Nguyen, *Microfluid. Nanofluidics* **2020**, *24*, 1-15.
[15] C. H. Ooi, N.-T. Nguyen, *Microfluid Nanofluidics* **2015**, *19*, 483-495.
[16] J. Jin, C. H. Ooi, K. R. Sreejith, D. V. Dao, N.-T. Nguyen, *Phys. Rev. Appl.* **2019**, *11*, 044059.
[17] C. H. Ooi, J. Jin, A. V. Nguyen, G. M. Evans, N.-T. Nguyen, *Microfluid. Nanofluidics* **2018**, *22*, 142.
[18] X. Fu, Y. Zhang, H. Yuan, B. P. Binks, H. C. Shum, *ACS Appl. Mater. Interfaces* **2018**, *10*, 34822-34827.
[19] Y. Zhang, X. Fu, W. Guo, Y. Deng, B. P. Binks, H. C. Shum, *Lab Chip* **2019**, *19*, 3526-3534.
[20] M. K. Khaw, C. H. Ooi, F. Mohd-Yasin, A. V. Nguyen, G. M. Evans, N.-T. Nguyen, *Microfluid. Nanofluidics* **2017**, *21*, 1-12.
[21] M. K. Khaw, C. H. Ooi, F. Mohd-Yasin, R. Vadivelu, J. St John, N.-T. Nguyen, *Lab Chip* **2016**, *16*, 2211-2218.
[22] M. Frenkel, V. Danchuk, V. Multanen, I. Legchenkova, Y. Bormashenko, O. Gendelman, E. Bormashenko, *Langmuir* **2018**, *34*, 6388-6395.
[23] C. H. Ooi, A. Van Nguyen, G. M. Evans, O. Gendelman, E. Bormashenko, N.-T. Nguyen, *RSC Adv.* **2015**, *5*, 101006-101012.
[24] E. Bormashenko, Y. Bormashenko, R. Grynyov, H. Aharoni, G. Whyman, B. P. Binks, *J. Phys. Chem. A C* **2015**, *119*, 9910-9915.
[25] N. Kavokine, M. Anyfantakis, M. Morel, S. Rudiuk, T. Bickel, D. Baigl, *Angew. Chem. Int. Ed.* **2016**, *55*, 11183-11187.
[26] B. Solomon, in *Advances in Biochemical Engineering, Volume 10*, Springer, **1978**, pp. 131-177.
[27] S. L. Hii, J. S. Tan, T. C. Ling, A. B. Ariff, *Enzyme Res.* **2012**, *2012*.
[28] M. W. Kearsley, S. Z. Dziedzic, *Handbook of starch hydrolysis products and their derivatives*, Springer Science & Business Media, **1995**.

[29] B. E. Haissig, R. E. Dickson, *Physiol. Plant.* **1979**, *47*, 151-157.
[30] P. S. Chow, S. M. Landhäusser, *Tree Physiol.* **2004**, *24*, 1129-1136.
[31] Y. Higuchi, A. Ohashi, H. Imachi, H. Harada, *Water Sci. Technol.* **2005**, *52*, 259-266.
[32] U. Etxeberria, A. L. de la Garza, J. Campión, J. A. Martinez, F. I. Milagro, *Expert Opin. Ther. Targets* **2012**, *16*, 269-297.
[33] D. Yankov, E. Dobreva, V. Beschkov, E. Emanuilova, *Enzyme Microb. Technol.* **1986**, *8*, 665-667.
[34] V. Komolprasert, R. Y. Ofoli, *J. Chem. Technol.* **1991**, *51*, 209-223.
[35] H. Hargono, B. Jos, B. Budiyono, S. Sumardiono, S. Priyanto, K. Haryani, M. Zakaria, in *AIP Conference Proceedings, Vol. 2197*, AIP Publishing LLC, **2020**, p. 120001.
[36] V. Ernest, P. Shiny, A. Mukherjee, N. Chandrasekaran, *Carbohydr. Res.* **2012**, *352*, 60-64.
[37] K. Nakagawa, Y. Goto, *Chem Eng Process* **2015**, *91*, 35-42.
[38] T. Kochanė, I. Zabarauskė, L. Klimkevičienė, A. Strakšys, S. Mačiulytė, L. Navickaitė, S. Gailiūnaitė, S. Budrienė, *Int. J. Biol. Macromol.* **2020**, *144*, 544-552.
[39] S. Wang, X. Huang, C. Yang, *Lab Chip* **2011**, *11*, 2081-2087.
[40] H. Masuda, T. Horie, R. Hubacz, N. Ohmura, M. Shimoyamada, *Biosci. Biotechnol. Biochem.* **2017**, *81*, 755-761.
[41] Y.-E. Miao, H. K. Lee, W. S. Chew, I. Y. Phang, T. Liu, X. Y. Ling, *ChemComm* **2014**, *50*, 5923-5926.
[42] W. Gao, H. K. Lee, J. Hobley, T. Liu, I. Y. Phang, X. Y. Ling, *Angew. Chem.* **2015**, *127*, 4065-4068.
[43] E. Sato, M. Yuri, S. Fujii, T. Nishiyama, Y. Nakamura, H. Horibe, *ChemComm* **2015**, *51*, 17241-17244.
[44] Y. Zhao, Z. Xu, H. Niu, X. Wang, T. Lin, *Adv. Funct. Mater.* **2015**, *25*, 437-444.
[45] C. S. L. Koh, H. K. Lee, G. C. Phan-Quang, X. Han, M. R. Lee, Z. Yang, X. Y. Ling, *Angew. Chem.* **2017**, *129*, 8939-8943.
[46] N. M. Oliveira, C. R. Correia, R. L. Reis, J. F. Mano, *Adv. Healthc. Mater.* **2015**, *4*, 264-270.
[47] H. Li, P. Liu, G. Kaur, X. Yao, M. Yang, *Adv. Healthc. Mater.* **2017**, *6*, 1700185.
[48] S. K. Kohl, J. D. Landmark, D. F. Stickle, *J. Chem. Educ.* **2006**, *83*, 644.
[49] E. da Nobrega Gaiao, V. L. Martins, W. da Silva Lyra, L. F. de Almeida, E. C. da Silva, M. C. U. Araújo, *Anal. Chim. Acta* **2006**, *570*, 283-290.
[50] W. Wongwilai, S. Lapanantnoppakhun, S. Grudpan, K. Grudpan, *Talanta* **2010**, *81*, 1137-1141.
[51] A. Choodum, N. Nic Daeid, *Drug Test Anal.* **2011**, *3*, 277-282.
[52] M. B. Lima, S. I. E. Andrade, I. S. Barreto, L. F. Almeida, M. C. U. Araújo, *Microchem. J.* **2013**, *106*, 238-243.
[53] R. W. Ricci, M. Ditzler, L. P. Nestor, *J. Chem. Educ.* **1994**, *71*, 983.
[54] D. J. Soldat, P. Barak, B. J. Lepore, *J. Chem. Educ.* **2009**, *86*, 617.
[55] K. D. Pessoa, W. T. Suarez, M. F. dos Reis, M. d. O. K. Franco, R. P. L. Moreira, V. B. dos Santos, *Spectrochim. Acta A Mol. Biomol. Spectrosc.* **2017**, *185*, 310-316.
[56] J. Wang, Y. Li, Y. Tian, X. Xu, X. Ji, X. Cao, Z. Jin, *Starke* **2010**, *62*, 508-516.
[57] A. Choodum, P. Kanatharana, W. Wongniramaikul, N. N. Daeid, *Talanta* **2013**, *115*, 143-149.
[58] C. H. Ooi, E. Bormashenko, A. V. Nguyen, G. M. Evans, D. V. Dao, N.-T. Nguyen, *Langmuir* **2016**, *32*, 6097-6104.
[59] K. R. Sreejith, C. H. Ooi, D. V. Dao, N.-T. Nguyen, *RSC Adv.* **2018**, *8*, 15436-15443.
[60] B. Laborie, F. Lachaussée, E. Lorenceau, F. Rouyer, *Soft Matter* **2013**, *9*, 4822-4830.
[61] A. F. Stalder, T. Melchior, M. Müller, D. Sage, T. Blu, M. Unser, *Colloids Surf. A Physicochem. Eng. Asp.* **2010**, *364*, 72-81.
[62] L. Ma-Hock, A. Gamer, R. Landsiedel, E. Leibold, T. Frechen, B. Sens, M. Linsenbuehler, B. Van Ravenzwaay, *Inhal. Toxicol.* **2007**, *19*, 833-848.
[63] M. Shankar, R. Priyadharshini, P. Gunasekaran, *Biotechnol. Lett.* **2009**, *31*, 1197-1201.
[64] L. P. dos Santos Benedetti, V. B. dos Santos, T. A. Silva, E. Benedetti Filho, V. L. Martins, O. Fatibello-Filho, *Anal. Methods* **2015**, *7*, 4138-4144.
[65] N.-K. Nguyen, C. H. Ooi, P. Singha, J. Jin, K. R. Sreejith, H.-P. Phan, N.-T. Nguyen, *Processes* **2020**, *8*, 793.
[66] S. Dhital, A. K. Shrestha, M. J. Gidley, *Carbohydr. Polym.* **2010**, *82*, 480-488.
[67] A. Párkány-Gyárfás, L. Vámos-Vigyázó, *Starke* **1979**, *31*, 328-332.
[68] P. K. Robinson, *Essays Biochem.* **2015**, *59*, 1-41.
[69] R. Visvanathan, C. Jayathilake, R. Liyanage, *Food Chem.* **2016**, *211*, 853-859.

Entry for the Table of Contents

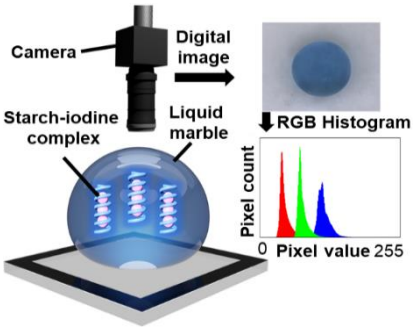

This paper presents a non-destructive and in situ digital-imaging colourimetry method based to monitor enzymatic.hydrolysis of starch in transparent liquid marbles. This method shows high sensitivity and repeatability, greatly enhancing the potential of liquid marble-based microreactor platform.